

# Rethinking Text Line Recognition Models

Daniel Hernandez Diaz  
Google Research  
dhernandezdiaz@google.com

Siyang Qin  
Google Research  
qinb@google.com

Reeve Ingle  
Google Research  
reeveingle@google.com

Yasuhisa Fujii  
Google Research  
yasuhisaf@google.com

Alessandro Bissacco  
Google Research  
bissacco@google.com

## Abstract

In this paper, we study the problem of text line recognition. Unlike most approaches targeting specific domains such as scene-text or handwritten documents, we investigate the general problem of developing a universal architecture that can extract text from any image, regardless of source or input modality. We consider two decoder families (Connectionist Temporal Classification and Transformer) and three encoder modules (Bidirectional LSTMs, Self-Attention, and GRCLs), and conduct extensive experiments to compare their accuracy and performance on widely used public datasets of scene and handwritten text. We find that a combination that so far has received little attention in the literature, namely a Self-Attention encoder coupled with the CTC decoder, when compounded with an external language model and trained on both public and internal data, outperforms all the others in accuracy and computational complexity. Unlike the more common Transformer-based models, this architecture can handle inputs of arbitrary length, a requirement for universal line recognition. Using an internal dataset collected from multiple sources, we also expose the limitations of current public datasets in evaluating the accuracy of line recognizers, as the relatively narrow image width and sequence length distributions do not allow to observe the quality degradation of the Transformer approach when applied to the transcription of long lines.

## 1 Introduction

Optical character recognition (OCR) is a crucial component of a wide range of practical applications, such as visual search, document digitization, autonomous vehicles, augmented reality (e.g., visual translation), and can increase the environmental awareness of visually impaired people [38]. In the last decade, increasing sophistication in OCR models has come hand-in-hand with a remarkable increase in

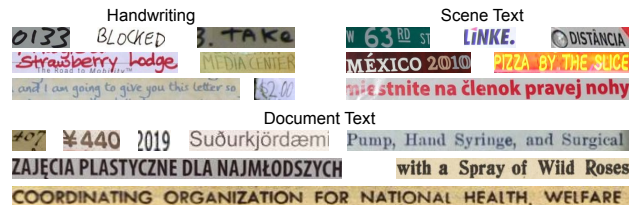


Figure 1: Example text line images in our Internal dataset, which contains handwriting, scene-text, and document text images of various lengths.

accuracy for various domains [17, 3, 8, 33].

Traditional approaches usually separate the text extraction task into two subproblems: *text detection* and *text recognition*. Text detection algorithms try to detect text instances (words or lines) in the input images, while text recognition models try to decode the textual content from cropped and rectified text patches. For scene (sparse) texts, the majority of the text spotting methods operate at the *word-level*, driven by the fact that most of the public datasets in the domain only provide word-level labeling. On the other hand, handwriting and dense text recognition systems typically adopt *lines* as the processing unit [3, 8, 24].

Despite the popularity of word-level systems for scene text recognition, operating at word-level could be suboptimal for a general purpose system supporting many scripts. First, for handwritten text, it is not always straightforward to separate words since detected boxes for neighboring words could partially overlap. Second, for dense printed documents, it is difficult to reliably detect a large amount of small and dense words. Third, it is challenging for detectors to separate words for scripts that do not separate words by spaces such as Chinese, Japanese, and Korean. Last but not least, word-level OCR models are more likely to miss punctuation and diacritic marks.

In this work, we consider a universal *line-based* OCR pipeline that can extract dense printed or handwritten text

as well as sparse scene-text with the goal of determining the optimal *text-line recognition* (TLR) model in this scenario. In such a pipeline, a separate text detection model is responsible for detecting and rectifying all lines of text in the image. As this step is outside the scope of this paper, we exclude from the analysis here public datasets with irregular scene text where detection and rectification are the main focus, such as [11]. In a line-based OCR system, *the recognizer needs to handle arbitrarily long text-lines effectively and efficiently*. This challenge has been overlooked by previous state-of-the-art word-based models. Public datasets (mostly word level) have relatively narrow image width and sequence length distributions (see Figure 5). At the same time, the design, performance and speed of TLR models depends on these variables. To understand these issues, we study TLR models trained on an internal dataset containing examples within a wide range of lengths and with a much larger symbol coverage (675 classes containing most of the symbols in Latin script and special characters, compared to alphanumeric characters used in majority of the public datasets). We found that techniques such as *image chunking* substantially alleviate the challenges posed by examples of wildly different sizes.

We explore a number of architectures for TLR and compare their accuracy and performance on the internal dataset. From this study emerge concrete recommendations for the design of universal, line-level, TLR systems. *We find that the model that uses a Self-Attention encoder [51] coupled with the Connectionist Temporal Classification (CTC) decoder [16], compounded with an explicit language model, outperforms all other models having both maximal text-line recognition accuracy and minimal complexity*. To the best of our knowledge, this model architecture has not been previously studied in the literature. It also fits within the overarching trend in machine learning of disposing of recurrent networks in favor of attention modules. More generally, encoder modules based on the self-attention mechanism emerge winners in our encoder comparison, regardless of decoder type. Our performance on widely used public datasets (including printed, handwritten and scene-text) are reported. We also report results of training this model on public datasets only, and show that even when using such a restricted train set accuracy is comparable to the widely used Transformer-based approach, and not far from significantly more complex state-of-the-art models.

To summarize, our contributions are four-fold:

- We fairly compare 9 different model design choices on an internal dataset and on a *universal* TLR task, pairing each of three encoders (Self-Attention, GRCL, and BiLSTM) to each of three decoders (CTC, CTC with LM and the Transformer decoder).
- We identify as the optimal model architecture a previ-

ously unstudied combination of Self-Attention encoding with CTC decoding. We found that this model yielded the top accuracy with low memory requirements and very good latency, making it an easy choice for low-resource environments.

- We propose the use of image chunking to ensure that the model works efficiently and effectively on arbitrary long input images without shrinking.
- We find that models based on the Transformer decoder have significant regression in quality if the image length is outside the length distribution of the training data.

## 2 Related Work

Handwriting and scene-text are usually treated separately in TLR, and most work in the literature focuses on one or the other. Nevertheless, models for these domains share many features in common. Generally speaking, they are designed around the use of a CNN for extracting a sequence of visual features, that is subsequently passed to an encoder/decoder network that outputs the labels.

For the case of Scene-Text Recognition (STR), an in-depth survey was recently carried out by Chen et al. [10]. Close in spirit to this paper is Baek et al. [2] in the domain of scene-text recognition. That work emphasized the inconsistencies among the public datasets typically used for training and evaluation in the literature, and was the first attempt to provide a uniform framework for the comparison of recognizer models. In their analysis, they include a transformation module, that preprocesses a potentially irregular input image before it is fed to the vision backbone. Compared to that work, this paper is a more focused effort. Assuming that images are rectified and fixing the vision backbone allows us to perform a more straightforward encoder/decoder comparison, also scanning over different encoder configurations.

CTC models for STR are well studied [46, 15, 49]. The seminal work by Shi et al. [46] proposed the standard, end-to-end backbone + encoder/decoder architecture for TLR tasks. Our Self-Attention / CTC model replaces the RNN in that work by a Self-Attention module. Sequence-to-Sequence (Seq2Seq) models with attention have become more prevalent for STR in recent years [59, 54, 45, 4, 30, 54], in part due to the advent of the Transformer architecture [51], that has allowed the field to loosen its ties to the recurrent connection. Sheng et al. [45] first applied the Transformer to STR [4]. Lee et al. [30] devised a novel 2D dynamic positional encoding method with impressive results. Other models with an initial rectification step [47, 2, 32, 48, 58] have been most successful in irregular STR. In particular, the drop in accuracy for longer lines

was noticed in [48]. Wang et al [55] combine a fully convolutional (FCN) encoder with an RNN decoder based on Gated Recurrent Units (GRU).

Modern methods for handwriting recognition (HWR) have been reviewed by Memon et al. [36]. Michael et al. [37] compare different attention mechanisms for Seq2Seq methods in the HWR domain. RNN encoders with CTC decoders have been customary for some time, with Long-Short Term Memory (LSTM) being the typical RNN cell of choice [6, 18, 39]. Multidimensional LSTM encoders have also been tried, e.g. [18, 52, 41]. Seq2Seq approaches to handwriting recognition including attention-based decoding have been catching up [37, 28, 40, 12, 5]. The difficulties with scaling handwriting recognition were tackled in [24].

### 3 Anatomy of a Text-Line Recognition Model

Most state-of-the-art TLR algorithms consists of three major components: a convolutional backbone to extract visual features; a sequential encoder which aggregates features from part or entire sequence; and finally a decoder which produces the final transcription given the encoder output. In this work, we study different combination of encoder and decoder with a fixed backbone and propose an optimal model architecture.

#### 3.1 Backbone

Similar to other vision tasks, a convolutional backbone network is used to extract relevant visual features from text-line images. Any of the many mainstream vision modules in the literature can be reused in principle as a TLR backbone; ResNet [20], Inception [50], and MobileNet-like [22, 44] networks are standard choices. Generally speaking, increasing the complexity of the backbone translates into moderate performance gains. In this work, we use a fixed backbone across all of the experiments while focusing on the question of finding the optimal encoder/decoder combination.

Our backbone is an isometric architecture [43] using Fused Inverted Bottleneck layers as building block, a variant of the Inverted Bottleneck layer [44] that replaces separable with full convolutions for higher model capacity and inference efficiency on modern accelerators [56]. Isometric architectures maintain constant internal resolution throughout all layers, allowing a low activation memory footprint and making it easier to customize the model to specialized hardware and achieve the highest utilization. Figure 3 illustrates the network in detail. It consists of a space-to-depth layer with block size 4, followed by 11 Fused Inverted Bottleneck layers with  $3 \times 3$  kernels and  $8 \times$  expansion rate with 64 output channels. A final fully convolutional resid-

ual block is applied to reduce the tensor height to 1, to be fed as input to the encoder network [24].

#### 3.2 Encoder

The backbone has a finite receptive field, which limits its ability to encode wide range context information. This makes it difficult to decode long sequences under challenging scenarios (e.g., handwritten text). Standard sequential encoders can be used to capture long-distance context features, making it a crucial component of the TLR model. In this work, we compare the following encoders:

**BiLSTM:** Bidirectional RNNs based on the LSTM cell [21] are natural candidates to capture long-range correlations in the output feature sequence of the backbone. In our comparison, we stack 1 to 3 LSTM layers, with each cell having 512 hidden units.

**Gated Recurrent Convolution Layer (GRCL):** GRCL was introduced in [53] and has demonstrated its effectiveness on OCR. Our GRCL encoder consists of 3 sets of repeated GRCL blocks. The convolutions in each of the 3 sets use [384, 256, 128] output filters and kernel widths (1-D convolution along width dimension) [3, 5, 7] respectively (Fig. 4). The basic layer in the repeated blocks of each set contains a convolutional gating mechanism, which uses a convolution with sigmoid activation to control information propagation from a convolution with ReLU activation. We compare 6 different variations where the number of GRCL blocks within each set varied from 1 to 6. Batch Renormalization [25] was used for each of the blocks and a dropout rate of 0.1 was applied in all the convolutional layers.

**Self-Attention:** The Self-Attention encoder, proposed in Vaswani et al. [51] has been widely used in numerous NLP and vision tasks. As an image-to-sequence task, text-line recognition is no exception. The Self-Attention encoder can effectively output features that summarize an entire sequence without making use of recurrent connections. The output of the backbone, with height dimension being removed ( $X \in \mathbb{R}^{n \times d}$ ), is fed to the encoder. The encoded feature  $Y$  is computed as:

$$Q = XW_q, \quad K = XW_k, \quad V = XW_v, \quad (1)$$

$$Y = \text{softmax} \left( \frac{QK^T}{\sqrt{d}} \right) V,$$

where  $W_q$ ,  $W_k$  and  $W_v$  are  $d \times d$  learned parameters which project the input sequence  $X$  into queries, keys and values respectively. The encoded feature  $Y$  is a convex combination of the computed values  $V$ , the similarity matrix is computed by the dot-product of queries and keys.

We use multi-head attention with 4 separate heads. The hidden size is set to 256. To prevent over-fitting, we apply dropout after each sub-layer with drop ratio 0.1. Sinusoidal relative positional encoding is added to make the encoder

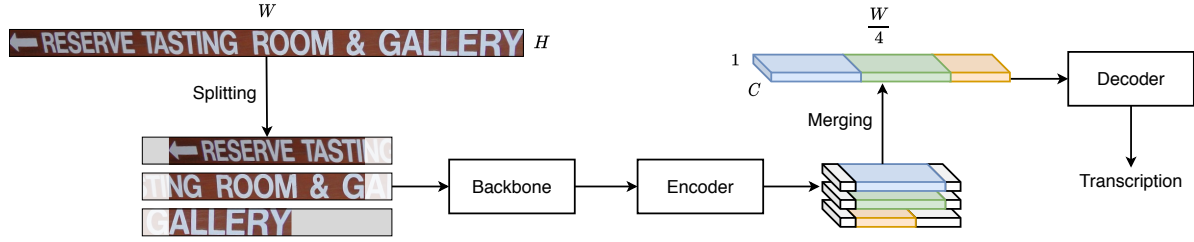


Figure 2: This figure shows the image chunking process. Input images are split into overlapping chunks with bidirectional padding before being fed to the backbone. The valid portions of the produced sequence features are concatenated before being fed to the decoder.

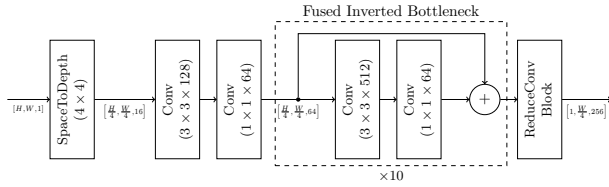


Figure 3: Backbone used in our experiments. We first reduce the resolution of input grayscale image by 4x with a space-to-depth operation, then we apply 11 Fused Inverted Bottleneck [56] layers with expansion rate 8 and 64 output channels, and use a residual convolution block to project the output into a tensor of height 1.

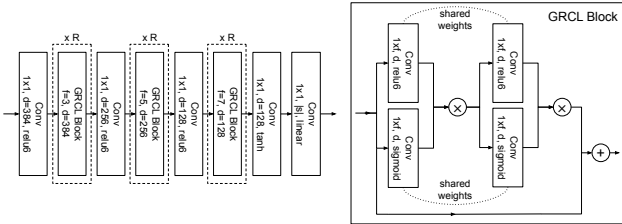


Figure 4: The GRCL encoder architecture.

position-aware. In our experiments, we compare the accuracy and complexity of different model variations by stacking  $k$  encoder layers with  $k \in \{4, 8, 12, 16, 20\}$ .

### 3.3 Decoder

Decoders take the encoded sequence features and try to decode its text content. CTC [16] and attention decoders are among the popular choices for text-line recognition. In this work, we compare the CTC decoder (with and without language model) and the Transformer decoder [51].

**CTC:** The CTC decoder was originally used in speech recognition, and researchers have had huge success adopting it to OCR tasks. The input encoded features can be viewed as vertical feature frames along the width dimen-

sion. The input is fed to a dense layer to obtain per-frame probabilities over possible labels. At inference time, we use a simple greedy CTC decoding strategy which removes all repeated symbols and all blanks from the per-frame predictions. Beam search decoding can be optionally used to consider multiple valid paths which are mapped to the same final output sequence. Our empirical study shows that beam search is not needed when CTC is paired with a powerful encoder such as the self-attention encoder.

**CTC w/ LM:** Incorporating an explicit language model on top of the logits from the optical model can significantly improve accuracy. We follow the approach described in [14] to form a log-linear model, combining the cost of CTC logits, the cost of a character-based  $N$ -gram language model, the cost of a character unigram prior, and transition costs defined for new characters, blank labels, and repeated characters. The weights of the feature functions were optimized using minimum error rate training [35].

**Transformer Decoder:** The Transformer decoder has become the decoder of choice for sequence prediction tasks such as machine translation. In our experiments, we incorporate a standard Transformer decoder with a stack of 8 repeated layers. In addition to self-attention and feed-forward layers, the decoder adds a third sub-layer which applies single-head attention over the encoded features (cross-attention to compute a context vector). The decoder’s hidden size is set to 256. Greedy decoding is applied at inference time. Per-step cross-entropy loss with label smoothing is used during training.

### 3.4 Chunking

Due to the dot-product attention in the self-attention layer, the model complexity and memory footprint of the encoder grows quadratically as a function of the image width. This can cause issues for inputs of large width. Shrinking wide images can avoid such issues but it will inevitably affect recognition accuracy, especially for narrow or closely-spaced characters.

We propose a simple yet effective chunking strategy to ensure that the model works well on arbitrarily wide input



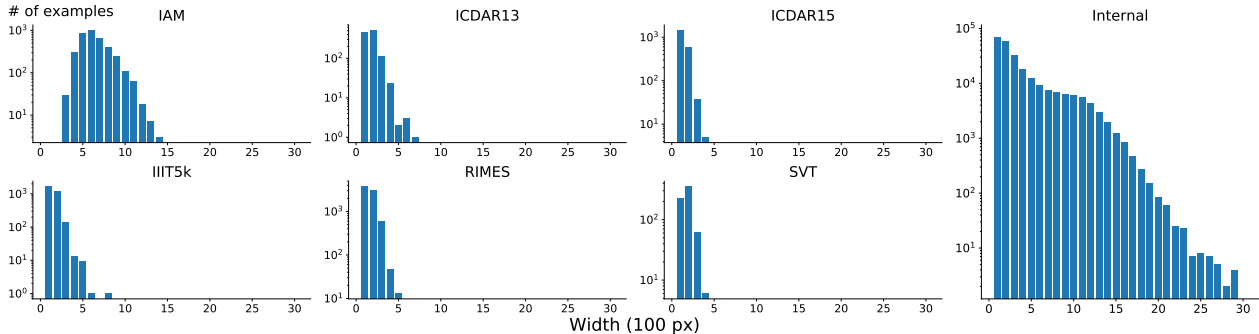


Figure 5: Height-normalized (40 px) distribution of text line images widths for the different datasets used in this work.

images without shrinking (see Figure 2), similar to [9]. We resize the input image to 40 pixels height, preserving the aspect ratio. Then the text-line is split into overlapping chunks with bidirectional padding to reduce possible boundary effects (note the last chunk has extra padding to ensure a uniform shape for batching purpose). We feed overlapping chunks into the backbone and self-attention encoder to produce sequence features for each chunk. Finally, we merge the valid regions back into a full sequence, removing the padding areas.

This approach splits long sequences into  $k$  shorter chunks, effectively reducing model complexity and memory usage by a factor of  $k$  for self-attention layers. This strategy is used both at training and inference time to keep a consistent behavior. Via a controlled experiment, we find no regression by applying chunking to the inputs. The aspect ratio of each chunk is set to 8 (i.e., 320 pixel width for 40 pixel height) to provide a reasonable amount of context information.

## 4 Experimental Setup

### 4.1 Datasets

To better train and evaluate TLR models for a line-based OCR engine with broad language support, we built an **Internal dataset** which contains both single words and long text-lines (see Figure 5). This dataset has multiple image sources, including synthetic text, scene-text, handwritten, documents, and photos reflecting some common phone camera use cases (translate, receipts, notes and memos). Scene-text training consists of the Uber-Text [60] and the OpenImages dataset [29] self-annotated with Google Cloud Vision TEXT\_DETECTION API [23]. Other images are from public sources - Flickr, Web pages - or collected through vendors specialized in crowdsourcing, which were given detailed instructions on how to collect the images to mimic photos taken by phone application users. The images

contain text from many Latin languages, with 675 symbols including punctuation and special characters, and were annotated by human raters with a transcription/verification iterative process seeded from the OCR predictions.

We also evaluate our models on six commonly used public benchmarks in the scene-text and handwriting domains, namely, IAM and RIMES for handwritten text, and IIIT5K, SVT, ICDAR13 and ICDAR 15 for scene-text (detailed descriptions of these datasets can be found in the Supplementary Material). Despite their wide usage, public datasets share two features that make them somewhat unrealistic, namely, *relatively narrow image-length distribution* and *lack of symbol coverage*. The height-normalized image width distribution of the test set of the public datasets is shown in the left panels in Figure 5. The IAM dataset lacks short lines while in the other word-level datasets long lines are missing.

### 4.2 Implementation Details

Models were trained on three different training data configurations : *Synth + Public*, *Internal*, and *Internal + Public*. Most of the analysis presented below corresponds to training on the *Internal* configuration, where only the internal dataset was used for training. To establish a qualitative comparison with other works, we also trained on the *Internal + Public* configuration, where data from *Internal* was combined with the training data from the public datasets (*Public*). These two were then mixed in a 9:4 ratio.

The *Synth + Public* runs are scene-text, public-data-only runs, that combine a merge of MJSynth[26, 27] and Synthtext[19] with the training data from the public datasets. The latter was further augmented 10 times by applying random distortions (affine, blur, noise, etc). During training, *synth* and *train* were mixed in a 10:3 ratio.

All of our models were trained and tested using grayscale images. Image chunking (Section 3.4) is applied to *CTC based models* at both training and inference time to efficiently handle arbitrarily long inputs. We normalize the im-

Table 1: Evaluation results on public handwriting and scene-text datasets of our best models and selected works. The ‘‘Rect.’’ column indicates whether the model includes a rectification module. ‘‘S-Attn’’, ‘‘Attn’’, and ‘‘Tfmr Dec.’’ stand for Self-Attention, Attention and Transformer Decoder respectively. ‘‘MJ’’, ‘‘ST’’ and ‘‘SA’’ stand for MJSynth[26, 27], SynthText [19] and SynthAdd [31] respectively.

	Rect.	Encoder / Decoder	Train Dataset	IAM ↓	RIMES ↓	IIIT5K ↑	SVT ↑	IC13 ↑	IC15 ↑
Bluche and Messina [6]	No	GCRNN/CTC	IAM (50k lexicon)	3.2	<b>1.9</b>	-	-	-	-
Michael et al. [37]	No	LSTM/LSTM w/Attn	IAM	4.87	-	-	-	-	-
Kang et al. [28]	No	Transformer	IAM	4.67	-	-	-	-	-
Bleeker and de Rijke [4]	No	Transformer	MJ + ST	-	-	94.7	89.0	93.4	75.7
Lu et al. [34]	No	Global Context Attn / Tfmr Dec.	MJ + ST + SA	-	-	95.0	90.6	95.3	79.4
Qiao et al. [42]	No	LSTM / LSTM + Attn	MJ + ST	-	-	94.4	90.1	93.3	77.1
Sheng et al. [45]	Yes	S-Attn / Attn	MJ + ST	-	-	93.4	89.5	91.8	76.1
Shi et al. [48]	Yes	LSTM / LSTM + Attn	MJ + ST	-	-	91.93	93.49	89.75	-
Wang et al. [55]	No	FCN / GRU	MJ + ST	6.4	2.7	94.3	89.2	93.9	74.5
SCATTER [32]	Yes	CNN / BiLSTM	MJ + ST + SA	-	-	93.9	92.7	94.7	<b>82.8</b>
Yu et al. [57]	No	Attn / Semantic Attn.	MJ + ST	-	-	94.8	91.5	95.5	82.7
Ours	No	S-Attn / CTC	MJ + ST + Public	-	-	92.06	87.94	92.15	72.36
	No	S-Attn / CTC + LM	MJ + ST + Public	-	-	93.63	91.50	93.61	74.77
	No	Transformer	MJ + ST + Public	-	-	93.93	92.27	93.88	77.08
	No	S-Attn / CTC	Internal	4.62	10.80	96.26	91.96	94.43	78.43
	No	S-Attn / CTC + LM	Internal	3.15	7.79	<b>96.83</b>	<b>94.59</b>	<b>95.98</b>	80.36
	No	Transformer	Internal	3.99	9.71	96.54	92.59	94.34	79.68
	No	S-Attn / CTC	Internal + Public	3.53	2.48	95.66	91.34	93.70	78.38
	No	S-Attn / CTC + LM	Internal + Public	<b>2.75</b>	1.99	96.43	93.66	95.25	79.92
	No	Transformer	Internal + Public	2.96	2.01	96.44	92.50	93.97	80.45

age height to 40 pixels while keeping the aspect ratio. For models which use the *Transformer decoder*, to prevent accuracy regression on long lines (Section 5.3), we feed fixed size images (resized and padded to  $1024 \times 40$ ) to the models. Since the image width is bounded, chunking strategy is not used for *Transformer decoder* based models.

The character-based  $N$ -gram language model for the CTC w/ LM decoder was trained from Web texts with stupid-backoff [7] and  $N$  was set to 9. The weights of the feature functions were tuned on the development portion of the internal dataset.

All the models are implemented in TensorFlow [1], trained using 32 TPU-v3 cores with a batch size of 1024. The SGD optimizer is used with momentum set to 0.9. We use a linear learning rate warm-up followed by stepped learning rate decay. Training iterations, initial learning rate, weight decay factor and global gradient clipping ratio are optimized for each model using grid search.

### 4.3 Evaluation Protocol

The handwriting datasets IAM and RIMES are evaluated using the case-sensitive Character Error Rate (CER), defined as the Levenshtein distance at the character level be-

tween the prediction and the ground truth, normalized by the ground truth length. For the scene-text public datasets, we use case-insensitive word prediction accuracy (WPA) to evaluate the recognition results as is customary. This is defined as  $1 - W$  where  $W$  is the Word Error Rate, defined through the Levenshtein distance, analogously to CER, but at the word level.

Evaluation on the internal test set, that includes images from the printed, handwritten and scene-text domains, is evaluated using both WPA and CER. No lexicon is used in any of our experiments.

## 5 Result Analysis

### 5.1 Encoder / Decoder Comparisons

Evaluation results on the *internal* test set are shown in Fig. 6 for CER and WPA, respectively. Within each figure, line color is used to indicate the encoder type: Self-Attention (pink), GRCL (green), or BiLSTM (blue). Alternatively, decoder type is indicated by the symbol: CTC (circle), CTC with LM (square), or Transformer Decoder (triangle).

The Self-Attention encoder (pink lines) is the most per-

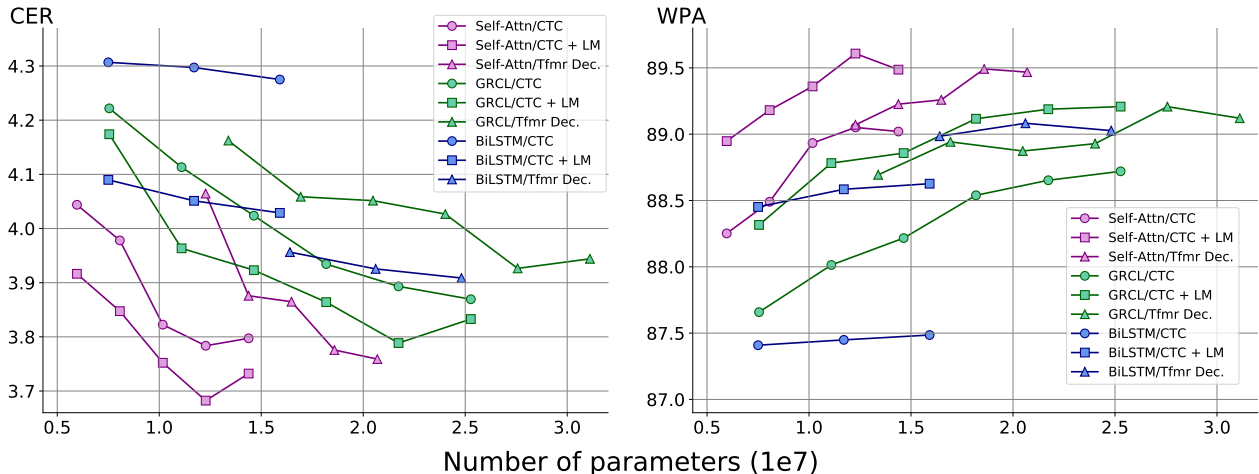


Figure 6: CERs and WPAs for the different encoder/decoder combinations evaluated on the internal test set. *Self-Attention*: 5 models are plotted per decoder corresponding to 4, 8, 12, 16, and 20 Self-Attention layers. *GRCL*: 6 models are plotted corresponding to the number of GRCL blocks per set, from 1 to 6. *BiLSTM*: Three models are plotted with increasing depth 1, 2, and 3.

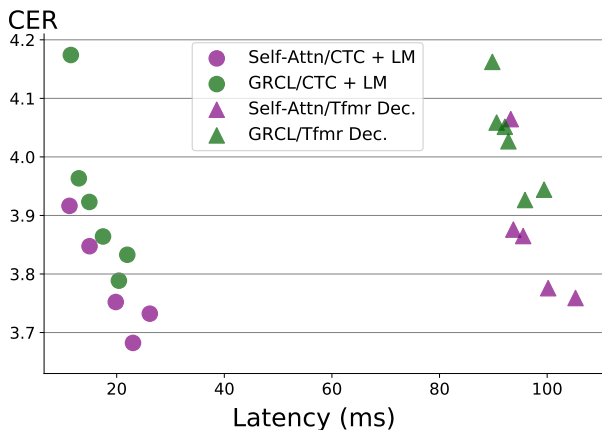


Figure 7: CER vs Latency for the non-recurrent models in Fig. 6. CTC decoding is 5-10 times faster. The LM adds a small overhead (1 ms). For all models, latency was computed on a NVIDIA V100 GPU card.

formant encoder irrespective of the decoder. With similar number of parameters, the CER for models with the Self-Attention encoder was  $\sim 2.5 - 10\%$  lower (relative) than for their GRCL and BiLSTM counterparts, translating into WPA gains of  $\sim 1\%$  absolute. Among all the models considered, the models with best CER and WPA for all three decoders were Self-Attention models.

CTC decoders compounded with an explicit LM achieve the best CER and WPA for the Self-Attention and GRCL encoders. The CER gains afforded by the LM applied to each of the CTC models considered, were relatively modest ( $<5\%$  relative for fixed number of parameters for Self-Attention and GRCL). There is a bigger improvement from

the LM for the BiLSTM encoder, but in that case, the Transformer Decoder outperformed CTC, an indication of the importance of the Attention mechanism in RNN architectures.

The clear winner overall is the model that combines a Self-Attention encoder, the CTC decoder with LM, using 12 Self-Attention layers or more. Our absolute best run, with 16 Self-Attention layers, produces a 4% relative CER improvement, with 8 million less parameters, over the second best model, a Self-Attention / Transformer Decoder with 20 encoder layers.

Different from other encoders, the BiLSTM encoder improved only slightly with more layers. This encoder is also more prone to overfitting and overall performs worse than the other two.

Without the explicit language model, CTC and the Transformer are overall competitive as decoders for the Self-Attention Module, but there are trade-offs. The CTC model has a better CER at the same number of parameters with similar WPA. However, the biggest Transformer model performs somewhat better in both metrics than the best CTC. Latency tells a different story. In Fig. 7, latencies for our non-recurrent models are represented for an input size of  $40 \times 320$ . CTC is 5 to 10 times faster than the Transformer decoder while increasing the capacity of the encoder or adding a LM contributes only a small overhead

## 5.2 Evaluation on Public Datasets

In Table 1 we show the performance on the test sets of the public datasets of our best models trained on *Synth + Public*, along with some of the best results reported in the

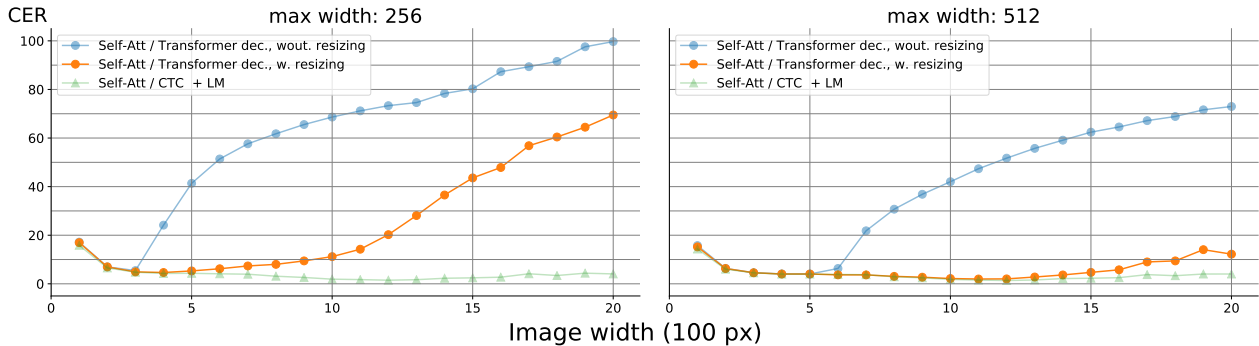


Figure 8: CER per 100 px bucket of height-normalized image width showing the impact of resizing during inference in the Transformer architecture trained with images up to 256px wide (left) and up to 512px wide (right). The Self-Attention / CTC + LM result is with the same training data is also shown for comparison.

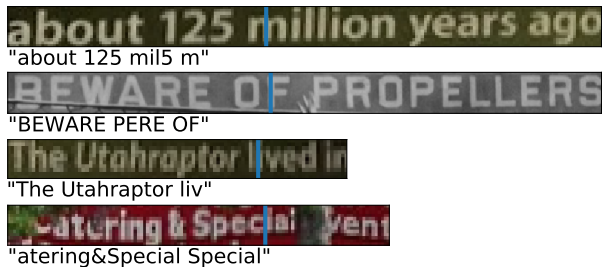


Figure 9: Failure cases for the Self-Attention / Transformer Decoder model, trained with images of maximum width 256 and evaluated with no resizing. Below each image, the TLR results. The vertical blue line denotes 256 pixel mark (height-normalized to 40 pixels)

literature. The table shows that in this training configuration, these models are competitive with SOTA, especially if one considers only models that do not include a rectification module. The Self-Attention/CTC model performs slightly worse than Self-Attention/Transformer in this configuration. Despite its small relative size, the inclusion of the *Public* dataset is key to achieve this performance; training on synthetic data only yields significantly worse results.

We also show the evaluation results for the *Internal* and *Internal + Public* training runs, on the test sets of the public datasets for both decoders. We stress that by presenting these results we do not intend to establish a comparison with SOTA, since the training data in this case differs from the public datasets typically used. No benefit was found from including the training portion of the scene-text public datasets in this training configuration. In fact, the runs that performed best on scene-text datasets corresponded to models trained with only *Internal* data. Conversely, adding the train sets of the handwritten public data have a substantial impact. This is most manifest for RIMES, in which the official training and test splits contain many examples with

repeated labels.

### 5.3 Resizing

In order to train the Transformer decoder models on TPUs, images are first resized to a fixed height and then either padded or anisotropically shrunk to a fixed maximum width  $M$ . Reducing  $M$  could in principle lead to faster training times, while potentially impacting performance, particularly for longer lines.

The performance changes with respect to  $M$  are shown in Fig. 8. In the figure we plot CER as a function of validation image width, grouped into buckets of 100 pixels. We considered two inference configurations differing on whether the validation images were resized to width  $M$  or not. The Self-Attention/CTC + LM result, when trained on the same data, is shown for comparison.

It is observed in Fig. 8 that the CERs drastically increase after  $M$  without resizing in both max widths. Fig. 9 shows typical failure cases without resizing. The recognizer appears to essentially stop decoding at the maximum width, often outputting the same characters observed around  $M$  repeatedly. Resizing the images to the maximum width at inference time alleviates the issue. However, there is a limitation with the approach. In our experiments, the accuracy started to noticeably degrade once the width of the image becomes longer than roughly  $2 \times M$ . In contrast, the accuracy of the CTC decoder is insensitive to the image width, which is another advantage of the CTC decoder.

## 6 Conclusions

In this work we investigated the performance of representative encoder/decoder architectures as universal text-line recognizers. In the decoder comparison, we found that CTC, compounded with a language model, yielded the overall superior performance. In the absence of a LM, CTC and



the Transformer are competitive, with CTC dominating in some cases (GRCL) and the Transformer in others (BiLSTM). On the other hand, in the encoder comparison, Self-Attention was the overall winner and both decoders were similarly accurate without LM. Interestingly, the unstudied Self-Attention/CTC + LM model, is our best. [13] showed that attention-based decoders can still benefit from an external language model. Investigations on the effectiveness of external language models with transformer decoders will be future work.

We also considered issues derived from the presence of long images in the distribution of examples. There are at least two new aspects that need to be considered, efficiency and performance. Long images affect the efficiency of models with the Self-Attention encoder due to quadratic scaling with image length. We showed that this problem can be solved for CTC models without performance loss by chunking the images. Training on images of fixed maximum width affects the performance on longer images of models that make use of the Transformer decoder. This problem can be alleviated, although not entirely eliminated, by resizing the images to the train width.

## References

- [1] Martín Abadi, Paul Barham, Jianmin Chen, Zhifeng Chen, Andy Davis, Jeffrey Dean, Matthieu Devin, Sanjay Ghemawat, Geoffrey Irving, Michael Isard, et al. Tensorflow: A system for large-scale machine learning. In *12th {USENIX} symposium on operating systems design and implementation ({OSDI} 16)*, pages 265–283, 2016. 6
- [2] Jeonghun Baek, Geewook Kim, Junyeop Lee, Sungrae Park, Dongyoon Han, Sangdoon Yun, Seong Joon Oh, and Hwal-suk Lee. What is wrong with scene text recognition model comparisons? *2019 IEEE/CVF International Conference on Computer Vision (ICCV)*, pages 4714–4722, 2019. 2
- [3] A. Bissacco, M. Cummins, Y. Netzer, and H. Neven. Photoocr: Reading text in uncontrolled conditions. In *2013 IEEE International Conference on Computer Vision*, pages 785–792, 2013. 1
- [4] Maurits Bleeker and Maarten de Rijke. Bidirectional scene text recognition with a single decoder. *arXiv preprint arXiv:1912.03656*, 2019. 2, 6
- [5] Theodore Bluche. Joint line segmentation and transcription for end-to-end handwritten paragraph recognition. In D. Lee, M. Sugiyama, U. Luxburg, I. Guyon, and R. Garnett, editors, *Advances in Neural Information Processing Systems*, volume 29, pages 838–846. Curran Associates, Inc., 2016. 3
- [6] T. Bluche and R. Messina. Gated convolutional recurrent neural networks for multilingual handwriting recognition. In *2017 14th IAPR International Conference on Document Analysis and Recognition (ICDAR)*, volume 01, pages 646–651, 2017. 3, 6
- [7] T. Brants, A. C. Popat, P. Xu, F. J. Och, and J. Dean. Large language models in machine translation. In *2007 Conference on Empirical Methods in Natural Language Processing (EMNLP)*, pages 858–867, 2007. 6
- [8] T. M. Breuel, A. Ul-Hasan, M. A. Al-Azawi, and F. Shafait. High-performance ocr for printed english and fraktur using lstm networks. In *2013 12th International Conference on Document Analysis and Recognition*, pages 683–687, 2013. 1
- [9] Kai Chen, Zhi-Jie Yan, , and Qiang Huo. A context-sensitive-chunk bptt approach to training deep lstm/blstm recurrent neural networks for offline handwriting recognition. In *2015 International Conference on Document Analysis and Recognition (ICDAR)*, pages 411–415, 2015. 5
- [10] Xiaoxue Chen, Lianwen Jin, Yuanzhi Zhu, Canjie Luo, and T. Wang. Text recognition in the wild: A survey. *ArXiv*, abs/2005.03492, 2020. 2
- [11] Chee Kheng Chng and Chee Seng Chan. Total-text: A comprehensive dataset for scene text detection and recognition. *CoRR*, abs/1710.10400, 2017. 2
- [12] Arindam Chowdhury and Lovekesh Vig. An Efficient End-to-End Neural Model for Handwritten Text Recognition. *arXiv e-prints*, page arXiv:1807.07965, July 2018. 3
- [13] Fuze Cong, Wenping Hu, Qiang Huo, and Li Guo. A comparative study of attention-based encoder-decoder approaches to natural scene text recognition. In *2019 International Conference on Document Analysis and Recognition (ICDAR)*, pages 916–921, 2019. 9

- [14] Y. Fujii, K. Driesen, J. Baccash, A. Hurst, and A. C. Popat. Sequence-to-label script identification for multilingual ocr. In *2017 International Conference on Document Analysis and Recognition (ICDAR)*, pages 161–168, 2017. 4
- [15] Yunze Gao, Yingying Chen, Jinqiao Wang, Ming Tang, and Hanqing Lu. Reading scene text with fully convolutional sequence modeling. *Neurocomputing*, 339:161 – 170, 2019. 2
- [16] Alex Graves, Santiago Fernández, Faustino Gomez, and Jürgen Schmidhuber. Connectionist temporal classification: Labelling unsegmented sequence data with recurrent neural networks. In *Proceedings of the 23rd International Conference on Machine Learning, ICML '06*, page 369–376, New York, NY, USA, 2006. Association for Computing Machinery. 2, 4
- [17] A. Graves, M. Liwicki, S. Fernández, R. Bertolami, H. Bunke, and J. Schmidhuber. A novel connectionist system for unconstrained handwriting recognition. *IEEE Transactions on Pattern Analysis and Machine Intelligence*, 31(5):855–868, 2009. 1
- [18] Alex Graves and Jürgen Schmidhuber. Offline handwriting recognition with multidimensional recurrent neural networks. In D. Koller, D. Schuurmans, Y. Bengio, and L. Bottou, editors, *Advances in Neural Information Processing Systems 21*, pages 545–552. Curran Associates, Inc., 2009. 3
- [19] Ankush Gupta, Andrea Vedaldi, and Andrew Zisserman. Synthetic data for text localisation in natural images. In *IEEE Conference on Computer Vision and Pattern Recognition*, 2016. 5, 6
- [20] Kaiming He, Xiangyu Zhang, Shaoqing Ren, and Jian Sun. Deep residual learning for image recognition. In *2016 IEEE Conference on Computer Vision and Pattern Recognition (CVPR)*, pages 770–778, 2016. 3
- [21] Sepp Hochreiter and Jürgen Schmidhuber. Long short-term memory. 9(8):1735–1780, Nov. 1997. 3
- [22] Andrew G. Howard, Menglong Zhu, Bo Chen, Dmitry Kalenichenko, Weijun Wang, Tobias Weyand, Marco Andreetto, and Hartwig Adam. Mobilenets: Efficient convolutional neural networks for mobile vision applications. *CoRR*, abs/1704.04861, 2017. 3
- [23] OCR in Google Cloud Vision API. <http://cloud.google.com/vision/docs/ocr>. 5
- [24] R. R. Ingle, Y. Fujii, T. Deselaers, J. Baccash, and A. C. Popat. A scalable handwritten text recognition system. In *2019 International Conference on Document Analysis and Recognition (ICDAR)*, pages 17–24, 2019. 1, 3
- [25] Sergey Ioffe. Batch renormalization: Towards reducing minibatch dependence in batch-normalized models. In I. Guyon, U. V. Luxburg, S. Bengio, H. Wallach, R. Fergus, S. Vishwanathan, and R. Garnett, editors, *Advances in Neural Information Processing Systems*, volume 30, pages 1945–1953. Curran Associates, Inc., 2017. 3
- [26] Max Jaderberg, Karen Simonyan, Andrea Vedaldi, and Andrew Zisserman. Synthetic data and artificial neural networks for natural scene text recognition. In *Workshop on Deep Learning, NIPS*, 2014. 5, 6
- [27] Max Jaderberg, Karen Simonyan, Andrea Vedaldi, and Andrew Zisserman. Reading text in the wild with convolutional neural networks. *International Journal of Computer Vision*, 116(1):1–20, jan 2016. 5, 6
- [28] Lei Kang, Pau Riba, Marçal Rusiñol, Alicia Fornés, and Mauricio Villegas. Pay attention to what you read: Non-recurrent handwritten text-line recognition, 2020. 3, 6
- [29] Alina Kuznetsova, Hassan Rom, Neil Alldrin, Jasper Uijlings, Ivan Krasin, Jordi Pont-Tuset, Shahab Kamali, Stefan Popov, Matteo Mallocci, Alexander Kolesnikov, and et al. The open images dataset v4. *International Journal of Computer Vision*, 128(7):1956–1981, Mar 2020. 5
- [30] Junyeop Lee, Sungrae Park, Jeonghun Baek, Seong Joon Oh, Seonghyeon Kim, and Hwalsuk Lee. On recognizing texts of arbitrary shapes with 2d self-attention. In *Proceedings of the IEEE/CVF Conference on Computer Vision and Pattern Recognition Workshops*, pages 546–547, 2020. 2
- [31] Hui Li, Peng Wang, Chunhua Shen, and Guyu Zhang. Show, attend and read: A simple and strong baseline for irregular text recognition. *Proceedings of the AAAI Conference on Artificial Intelligence*, 33(01):8610–8617, Jul. 2019. 6
- [32] Ron Litman, Oron Anshel, Shahar Tsiper, Roe Litman, Shai Mazor, and R. Manmatha. Scatter: Selective context attentional scene text recognizer. In *Proceedings of the IEEE/CVF Conference on Computer Vision and Pattern Recognition (CVPR)*, June 2020. 2, 6
- [33] Shangbang Long, Xin He, and Cong Yao. Scene text detection and recognition: The deep learning era. *International Journal of Computer Vision*, pages 1–24, 2020. 1
- [34] Ning Lu, Wenwen Yu, Xianbiao Qi, Yihao Chen, Ping Gong, and Rong Xiao. MASTER: multi-aspect non-local network for scene text recognition. *CoRR*, abs/1910.02562, 2019. 6
- [35] W. Macherey, F. J. Och, I. Thayer, and J. Uszkoreit. Lattice-based minimum error rate training for statistical machine translation. pages 725–734, 2008. 4
- [36] J. Memon, M. Sami, R. A. Khan, and M. Uddin. Handwritten optical character recognition (ocr): A comprehensive systematic literature review (slr). *IEEE Access*, 8:142642–142668, 2020. 3
- [37] J. Michael, R. Labahn, T. Grüning, and J. Zöllner. Evaluating sequence-to-sequence models for handwritten text recognition. In *2019 International Conference on Document Analysis and Recognition (ICDAR)*, pages 1286–1293, 2019. 3, 6
- [38] Leo Neat, Ren Peng, Siyang Qin, and Roberto Manduchi. Scene text access: A comparison of mobile ocr modalities for blind users. In *Proceedings of the 24th International Conference on Intelligent User Interfaces*, pages 197–207, 2019. 1
- [39] V. Pham, T. Bluche, C. Kermorvant, and J. Louradour. Dropout improves recurrent neural networks for handwriting recognition. In *2014 14th International Conference on Frontiers in Handwriting Recognition*, pages 285–290, 2014. 3
- [40] J. Poulos and Rafael Valle. Attention networks for image-to-text. *ArXiv*, abs/1712.04046, 2017. 3
- [41] J. Puigcerver. Are multidimensional recurrent layers really necessary for handwritten text recognition? In *2017 14th IAPR International Conference on Document Analysis and Recognition (ICDAR)*, volume 01, pages 67–72, 2017. 3

- [42] Zhi Qiao, Xugong Qin, Yu Zhou, Fei Yang, and Weiping Wang. Gaussian constrained attention network for scene text recognition, 2020. [6](#)
- [43] Mark Sandler, Jonathan Baccash, Andrey Zhmoginov, and Andrew Howard. Non-discriminative data or weak model? on the relative importance of data and model resolution, 2019. [3](#)
- [44] M. Sandler, A. Howard, M. Zhu, A. Zhmoginov, and L. Chen. Mobilenetv2: Inverted residuals and linear bottlenecks. In *2018 IEEE/CVF Conference on Computer Vision and Pattern Recognition*, pages 4510–4520, 2018. [3](#)
- [45] Fenfen Sheng, Zhineng Chen, and Bo Xu. NRTR: A no-recurrence sequence-to-sequence model for scene text recognition. *CoRR*, abs/1806.00926, 2018. [2](#), [6](#)
- [46] B. Shi, X. Bai, and C. Yao. An end-to-end trainable neural network for image-based sequence recognition and its application to scene text recognition. *IEEE Transactions on Pattern Analysis & Machine Intelligence*, 39(11):2298–2304, nov 2017. [2](#)
- [47] Baoguang Shi, Xinggang Wang, Pengyuan Lyu, Cong Yao, and Xiang Bai. Robust scene text recognition with automatic rectification. In *Proceedings of the IEEE Conference on Computer Vision and Pattern Recognition (CVPR)*, June 2016. [2](#)
- [48] B. Shi, M. Yang, X. Wang, P. Lyu, C. Yao, and X. Bai. Aster: An attentional scene text recognizer with flexible rectification. *IEEE Transactions on Pattern Analysis and Machine Intelligence*, 41(9):2035–2048, 2019. [2](#), [3](#), [6](#)
- [49] Bolan Su and Shijian Lu. Accurate scene text recognition based on recurrent neural network. In Daniel Cremers, Ian Reid, Hideo Saito, and Ming-Hsuan Yang, editors, *Computer Vision – ACCV 2014*, Cham, 2015. Springer International Publishing. [2](#)
- [50] C. Szegedy, Wei Liu, Yangqing Jia, P. Sermanet, S. Reed, D. Anguelov, D. Erhan, V. Vanhoucke, and A. Rabinovich. Going deeper with convolutions. In *2015 IEEE Conference on Computer Vision and Pattern Recognition (CVPR)*, pages 1–9, 2015. [3](#)
- [51] Ashish Vaswani, Noam Shazeer, Niki Parmar, Jakob Uszkoreit, Llion Jones, Aidan N Gomez, Łukasz Kaiser, and Illia Polosukhin. Attention is all you need. In I. Guyon, U. V. Luxburg, S. Bengio, H. Wallach, R. Fergus, S. Vishwanathan, and R. Garnett, editors, *Advances in Neural Information Processing Systems 30*, pages 5998–6008. Curran Associates, Inc., 2017. [2](#), [3](#), [4](#)
- [52] P. Voigtlaender, P. Doetsch, and H. Ney. Handwriting recognition with large multidimensional long short-term memory recurrent neural networks. In *2016 15th International Conference on Frontiers in Handwriting Recognition (ICFHR)*, pages 228–233, 2016. [3](#)
- [53] Jianfeng Wang and Xiaolin Hu. Gated recurrent convolution neural network for ocr. In I. Guyon, U. V. Luxburg, S. Bengio, H. Wallach, R. Fergus, S. Vishwanathan, and R. Garnett, editors, *Advances in Neural Information Processing Systems 30*, pages 335–344. Curran Associates, Inc., 2017. [3](#)
- [54] S. Wang, Y. Wang, X. Qin, Q. Zhao, and Z. Tang. Scene text recognition via gated cascade attention. In *2019 IEEE International Conference on Multimedia and Expo (ICME)*, pages 1018–1023, 2019. [2](#)
- [55] Tianwei Wang, Yuanzhi Zhu, Lianwen Jin, Canjie Luo, Xiaoxue Chen, Yaqiang Wu, Qianying Wang, and Mingxiang Cai. Decoupled attention network for text recognition. In *The Thirty-Fourth AAAI Conference on Artificial Intelligence, AAAI 2020, The Thirty-Second Innovative Applications of Artificial Intelligence Conference, IAAI 2020, The Tenth AAAI Symposium on Educational Advances in Artificial Intelligence, EAAI 2020, New York, NY, USA, February 7-12, 2020*, pages 12216–12224. AAAI Press, 2020. [3](#), [6](#)
- [56] Yunyang Xiong, Hanxiao Liu, Suyog Gupta, Berkin Akin, Gabriel Bender, Pieter-Jan Kindermans, Mingxing Tan, Vikas Singh, and Bo Chen. MobileDets: Searching for object detection architectures for mobile accelerators, 2020. [3](#), [4](#)
- [57] Deli Yu, Xuan Li, Chengquan Zhang, Tao Liu, Junyu Han, Jingtuo Liu, and Errui Ding. Towards accurate scene text recognition with semantic reasoning networks. In *Proceedings of the IEEE/CVF Conference on Computer Vision and Pattern Recognition*, pages 12113–12122, 2020. [6](#)
- [58] F. Zhan and S. Lu. Esir: End-to-end scene text recognition via iterative image rectification. In *2019 IEEE/CVF Conference on Computer Vision and Pattern Recognition (CVPR)*, pages 2054–2063, 2019. [2](#)
- [59] Jiaxin Zhang, Canjie Luo, Lianwen Jin, Tianwei Wang, Ziyang Li, and Weiyang Zhou. Sahan: Scale-aware hierarchical attention network for scene text recognition. *Pattern Recognition Letters*, 136:205 – 211, 2020. [2](#)
- [60] Ying Zhang, Lionel Gueguen, Ilya Zharkov, Peter Zhang, Keith Seifert, and Ben Kadlec. Uber-text: A large-scale dataset for optical character recognition from street-level imagery. In *SUNw: Scene Understanding Workshop - CVPR 2017*, Hawaii, U.S.A., 2017. [5](#)